Available online at www.sciencedirect.com

ScienceDirect

Physica D 237 (2008) 1894–1904

PHYSICA D

www.elsevier.com/locate/physd

The three-dimensional Euler equations: Where do we stand?

J.D. Gibbon*

Department of Mathematics, Imperial College London, London SW7 2AZ, United Kingdom

Available online 1 November 2007

Abstract

The three-dimensional Euler equations have stood for a quarter of a millenium as a challenge to mathematicians and physicists. While much has been discovered, the nature of solutions is still largely a mystery. This paper surveys some of the issues, such as singularity formation, that have cost so much effort in the last 25 years. In this light we review the Beale–Kato–Majda theorem and its consequences and then list some of the results of numerical experiments that have been attempted. A different line of endeavour focuses on work concerning the pressure Hessian and how it may be used and modelled. The Euler equations are finally discussed in terms of their membership of a class of general Lagrangian evolution equations. Using Hamilton's quaternions, these are reformulated in an elegant manner to describe the motion and rotation of fluid particles.

PACS: 47.10.A-; 47.15.ki

Keywords: Vorticity; Singularities; Hessian; Quaternions

1. Introduction

The Apocryphal book Ecclesiasticus says [1]

Let us now praise famous men, and our fathers that begat us. . . . All these were honoured in their generations, and were the glory of their times . . .

and goes on to conclude in the same passage

There be of them that have left a name behind them, that their praises might be reported.

Leonhard Euler was certainly honoured in his own generation and has left a name behind him in manifold and diverse ways. Not only has his star shone ever more brightly, but the equations of inviscid fluid dynamics that bear his name have also stood the test of a quarter of a millennium of investigation and still stand proudly today as a challenge to the mathematical, physical and engineering sciences [2]. The incompressible Euler equations have a deceptively innocent simplicity about them; indeed their siren song has tempted many young scientists, somewhat like Ulysses, towards the twin rocks called Frustration and Despair. After a career spent in puzzlement, the sadder but wiser researcher is forced to admit how subtle and difficult they are.

They can be expressed as a set of partial differential equations relating the velocity vector field $\boldsymbol{u}(\boldsymbol{x}, t)$ to the pressure $p(\boldsymbol{x}, t)$

$$\frac{\mathrm{D}\boldsymbol{u}}{\mathrm{D}t} = -\nabla p, \tag{1}$$

$$\frac{\mathrm{D}}{\mathrm{D}t} = \frac{\partial}{\partial t} + \boldsymbol{u}\cdot\nabla, \tag{2}$$

where $\operatorname{div}\boldsymbol{u} = 0$ is an incompressibility condition. Applying this condition to (1) and (2) forces the pressure to satisfy an elliptic equation $-\Delta p = u_{i,j}u_{j,i}$ that involves products of velocity gradients. This can also be re-expressed in terms of the strain matrix $S_{ij} = \frac{1}{2}(u_{i,j} + u_{j,i})$

$$-\Delta p = u_{i,j}u_{j,i} = \mathrm{Tr}\left(S^2\right) - \frac{1}{2}\omega^2. \tag{3}$$

The vorticity $\boldsymbol{\omega} = \operatorname{curl}\boldsymbol{u}$ obeys the Euler equations in their vorticity form

$$\frac{\mathrm{D}\boldsymbol{\omega}}{\mathrm{D}t} = \boldsymbol{\omega}\cdot\nabla\boldsymbol{u}. \tag{4}$$

* Tel.: +44 207 594 8504.
E-mail address: j.d.gibbon@ic.ac.uk.

0167-2789/$ - see front matter © 2007 Elsevier B.V. All rights reserved.
doi:10.1016/j.physd.2007.10.014

On a domain Ω, the energy $\int_\Omega |\boldsymbol{u}|^2 \mathrm{d}V$, the circulation $\int_C \boldsymbol{u} \cdot \mathrm{d}\boldsymbol{r}$ and the helicity $\int_\Omega \boldsymbol{u} \cdot \boldsymbol{\omega} \mathrm{d}V$ are all conserved; for historical observations on these quantities see [3].

Given the large volume of work on the two- and three-dimensional Euler equations, it would be vacuous to attempt to cover every aspect, but there are certain significant areas I wish to mention before moving on to other material in more detail. It is appropriate at this point to pay tribute to Viktor Yudovich who died in the Spring of 2006 and whose work on establishing weak solutions in the two-dimensional case made him one of the fathers of modern Euler analysis [4]. Unfortunately these solutions have no such counterpart in the three-dimensional case for arbitrary initial data in L^2, which would be the analogue of Leray solutions [5]. Their absence creates difficulties for the mathematician who wishes to make each step rigorous. In these terms, standard manipulations of the three-dimensional Euler equations have to be undertaken in a formal way. Along-side this, but closer in spirit to two-dimensional Euler analysis, is a sizable literature on weak and distributional formulations of vortex sheets and the numerical methods needed to describe their roll-up. These areas have their own specialist literature which can be found in the book by Majda and Bertozzi [6].

A particular area deserving of special mention is what is now referred to as "topological fluid dynamics". Inspired by ideas based on the conservation of helicity [7–9], Moffatt [10] studied the Euler equations and those of ideal magneto-hydrodynamics through the respective tangling and knotting of vortex lines and of magnetic field lines. Together with the book by Arnold and Khesin [11], which takes a more general mathematical approach, the distillation of almost 40 years of literature in references [10,12–15] should be read by every graduate student wishing to study this area.

2. The difference between the three- and two-dimensional cases

2.1. Vortex stretching

Let us formally consider the vortex stretching term $\boldsymbol{\omega} \cdot \nabla \boldsymbol{u}$ in (4) in more detail for the three-dimensional case. Splitting the velocity gradient matrix $\nabla \boldsymbol{u} = \{u_{i,j}\}$ into its symmetric and anti-symmetric parts gives

$$(\nabla \boldsymbol{u})\boldsymbol{h} = S\boldsymbol{h} + \frac{1}{2}\boldsymbol{\omega} \times \boldsymbol{h}, \tag{5}$$

where $\boldsymbol{h}$ is an arbitrary 3-vector. It is then easy to see that if $\boldsymbol{h} \equiv \boldsymbol{\omega}$ then the anti-symmetric part plays no role and (4) becomes

$$\frac{\mathrm{D}\boldsymbol{\omega}}{\mathrm{D}t} = S\boldsymbol{\omega}. \tag{6}$$

At first glance this appears to be a deceptively simple eigenvalue problem, except the three eigenvalues $\{\lambda_1, \lambda_2, \lambda_3\}$ of S are functions of space-time and are subject to the divergence-free constraint $\lambda_1 + \lambda_2 + \lambda_3 = 0$. Rapid changes of size and sign in λ_i, subject to this constraint, could violently stretch or compress the vorticity field in various directions, thereby producing the fine-scale vortical structures that are so familiar in the graphical output of three-dimensional numerical computations.

In two dimensions, however, $\boldsymbol{\omega}$ is perpendicular to the plane in which the gradient lies, and so the vortex stretching term $\boldsymbol{\omega} \cdot \nabla \boldsymbol{u} = 0$. This observation illustrates the fact that the absence or presence of the vortex stretching term makes a huge difference to the vortical behaviour and suggests that the two and three-dimensional cases are fundamentally different equations with significantly different properties.

As its title suggests, this paper concentrates mainly on the three-dimensional case, but some short remarks on the two-dimensional and two-and-a-half-dimensional cases are nevertheless in order.

2.2. The two-dimensional Euler equations

Because $\boldsymbol{\omega} \cdot \nabla \boldsymbol{u} = 0$ in two-dimensions, (4) becomes

$$\frac{\mathrm{D}\boldsymbol{\omega}}{\mathrm{D}t} = 0, \tag{7}$$

and thus $\boldsymbol{\omega}$ is a constant of the motion. One difficult and subtle problem is the evolution of a two-dimensional patch of vorticity with an initially smooth closed boundary, inside which $\boldsymbol{\omega} =$ const. Whether the boundary of the patch remains smooth if it starts smooth, or whether it develops a cusp in a finite time, was once a long-standing open question until Chemin [16] proved that if an initial boundary Γ_0 is smooth (C^r for $r > 1$) then Γ_t must remain smooth. The bounds are parameterized by a double exponential in time so it is possible that numerical computations might suggest the development of a cusp even though the proof rules one out. An alternative proof using methods of harmonic analysis by Bertozzi and Constantin [17] can also be seen in [6].

2.3. The two-and-a-half-dimensional Euler equations

The class of solutions of the three-dimensional Euler equations that take the form

$$\boldsymbol{U}_{3D}(x, y, z, t) = \{\boldsymbol{u}(x, y, t), z\gamma(x, y, t)\} \tag{8}$$

are usually referred to as being of "two-and-a-half-dimensional type" because the predominant two-dimensional part in the cross-section is stretched linearly into a third dimension. This class of solutions generalizes those investigated some years ago by Stuart [18] who found a class of solutions in which two independent spatial variables were taken to be linear. The resulting partial differential equation has solutions that develop a singularity in a finite time. Eq. (8) suggests that an appropriate domain should be infinite in z with a circular periodic cross-section $\mathcal{A}$ of radius L. The two-dimensional velocity field $\boldsymbol{u}(x, y, t)$ in Eq. (8) satisfies

$$\frac{\mathrm{D}\boldsymbol{u}}{\mathrm{D}t} = -\nabla p \tag{9}$$

while $\operatorname{div} \boldsymbol{u} = -\gamma$. The fact that $\operatorname{div} \boldsymbol{u} \neq 0$ means that $\boldsymbol{u}(x, y, t)$ does not fully satisfy the two-dimensional Euler equations and that fluid particles in any one cross-section are allowed to move through any other. $\gamma(x, y, t)$ itself satisfies

$$\frac{D\gamma}{Dt} + \gamma^2 = \frac{2}{\pi L^2}\int_{\mathcal{A}} \gamma^2 dA. \tag{10}$$

While the above formulation can be found in Ohkitani and Gibbon [19], it turns out a time-independent form of these equations was written down long ago by Oseen in an appendix to a double paper [20]. He took the idea no further, however. Ohkitani and Gibbon [19] showed numerically $\gamma \to -\infty$ in a finite time. Later, using Lagrangian arguments, Constantin [21] proved analytically that $\gamma \to \pm\infty$. In other words, the blow-up is two-sided and occurs in different parts of the cross-section $\mathcal{A}$. An important point to note is that this blow-up does not represent a true singularity in the fluid, for this would need infinite energy to draw particles from infinity. More realistically, it suggests the full system will not sustain a solution of the form of (8) beyond the singular time. Before this singular time, the solution physically represents a class of stretched Burgers vortices: when $\gamma \to +\infty$ the vortex is tube-like but when $\gamma \to -\infty$ the vortex is ring-like [19]. This orthogonal pair of vortices, locked non-linearly together, has only a finite lifetime and is destroyed by the two-sided blow-up. Moreover, the finite lifetime of these vortices is consistent with experimental observations in turbulent flows where, among the collective set, individual tubes squirm around and then vanish after a short period [22–24]. A class of analytical singular solutions of a special case of (8)–(10) has been found using the method of characteristics [25].

3. The three-dimensional Euler singularity problem

One of the great open questions in mathematical fluid dynamics today is whether the incompressible three-dimensional Euler equations develop a singularity in the vorticity field in a finite time. Opinion is largely divided on the matter with strong positions taken on each side. That the vorticity accumulates rapidly from a variety of initial conditions is not under dispute, but whether the accumulation is sufficiently rapid to manifest singular behaviour or whether the growth is merely exponential, or double-exponential, has not been answered definitively. The interest in singularities comes from many directions. Physically their formation may signify the onset of turbulence and may be a mechanism for energy transfer to small scales: see the companion article in this issue by Eyink [26]. Numerically they require very special methods and are thus a challenge to computational fluid dynamics. Finally, the question is of interest to mathematicians because of the question of global existence of solutions. This section reviews some of the theoretical and computational work of the last 25 years.

3.1. The Beale–Kato–Majda Theorem

Work on the existence of solutions culminated in what is known as the Beale–Kato–Majda Theorem [27]. It was originally proved on an infinite domain with solutions decaying sufficiently rapidly at infinity but the domain Ω could easily be taken to be periodic instead. We refer the reader to the recent review by Bardos and Titi [28]. There are various ways of stating the result but the following form will be used:

Theorem 1. *There exists a global solution of the 3D Euler equations* $\boldsymbol{u} \in C([0,\infty]; H^s) \cap C^1([0,\infty]; H^{s-1})$ *for* $s \geq 3$ *if, for every* $T > 0$

$$\int_0^T \|\boldsymbol{\omega}(\cdot,\tau)\|_{L^\infty(\Omega)} d\tau < \infty. \tag{11}$$

Ferrari [29] has also proved a version of this result on boundary conditions where $\boldsymbol{u}\cdot\hat{\boldsymbol{n}} = 0$. Kozono and Taniuchi [30] have more recently proved a version of this theorem in the BMO-norm (bounded mean oscillations) which is weaker than the L^∞-norm. For literature on variations of the BKM theorem see Ponce [31] and Chae [32–35].

There are several other points to note about this important result which settled several outstanding questions. First it says that only one object, the maximum norm, needs to be monitored in a numerical calculation. Second, this object is different from the point-wise enstrophy $\|\boldsymbol{\omega}\|_{L^2(\Omega)}$. Having the latter bounded guarantees the regularity of the three-dimensional Navier–Stokes equations but this is not enough for Euler; it is theoretically possible that $\|\boldsymbol{\omega}\|_{L^2(\Omega)}$ could remain finite but $\|\boldsymbol{\omega}\|_{L^\infty(\Omega)}$ blow up.

Third, the result also says something subtle about the nature of singular behaviour in numerical experiments. For instance, say that a numerical integration of the three-dimensional Euler equations produces data that suggests that the maximum norm grows like ($\beta > 0$)

$$\|\boldsymbol{\omega}(\cdot,t)\|_{L^\infty(\Omega)} \sim (T-t)^{-\beta}. \tag{12}$$

The theorem says that the solution remains regular, including $\|\boldsymbol{\omega}\|_{L^\infty(\Omega)}$ itself, if the time integral in (11) is finite. If the observed value of β lies in the range $0 < \beta < 1$, however, the time integral of (12) is finite and thus the theorem contradicts the numerical result. The observed singularity is likely to be an artefact of the numerics. The theorem contains no information on whether a singularity occurs but it does say that β must satisfy $\beta \geq 1$ for the singularity to be genuine.

3.2. Numerical search for singularities

There have been many numerical experiments over the last quarter of a century that have attempted to determine, from specific initial data, whether the vorticity field in the three-dimensional Euler equations develops a singularity in a finite time. At this stage I would like to pay tribute to Richard Pelz (1957–2002), who was a much-valued and gentlemanly member of our community. His interests lay in the potential development of Euler singularities under Kida's high-symmetry conditions [36]. His work and that with his collaborators is referenced in the list below. Shigeo Kida has also edited a volume in his memory [37]. The list is a revised and updated version of one originally compiled by Rainer Grauer of Bochum. The "yes/no" in each item refers to whether the authors detected the development of a singularity from their initial data. Except for item 2 all calculations refer to the 3D Euler equations.

1. Morf, Orszag and Frisch [38–40]: complex time singularities of the 3D Euler equations were studied using Padé-approximants. Singularity; yes.
2. Pauls, Matsumoto, Frisch and Bec [41]: this paper is a recent study of complex singularities of the 2D Euler equations and contains a good list of references for the student.
3. Chorin [42]: Vortex–method. Singularity; yes.
4. Brachet, Meiron, Nickel, Orszag and Frisch [43]: Taylor–Green calculation. Singularity; no.
5. Siggia [44]: Vortex–filament method; became anti–parallel. Singularity; yes.
6. Pumir and Siggia [45]: results from their adaptive grid method showed a tendency to develop quasi-two-dimensional structures with exponential growth of vorticity. Singularity; no.
7. Bell and Marcus [46]: the evolution of a perturbed vortex tube was studied using a projection method with 128^3 mesh points; amplification of vorticity by 6. Singularity; yes.
8. Brachet, Meneguzzi, Vincent, Politano and Sulem [47]: pseudospectral code, Taylor–Green vortex, with a resolution of 864^3. They achieved an amplification of vorticity by 5. Singularity; no.
9. Kerr [48,49]: Chebyshev polynomials with anti–parallel initial conditions; resolution $512^2 \times 256$. Amplification of vorticity by 18. Observed vorticity growth $\|\boldsymbol{\omega}\|_{L^\infty(\Omega)} \sim (T-t)^{-1}$. Singularity; yes.
10. Between 1994–2001 Boratav and Pelz [50,51], Pelz and Gulak [53] and Pelz [52,54] performed a series of 1024^3 grid-point simulations under Kida's high-symmetry condition. Singularity; yes.
    The recent memorial issue for Pelz [37] contains:
    (a) Cichowlas and Brachet [55]: Singularity; no.
    (b) Gulak and Pelz [56]: Singularity; yes.
    (c) Pelz and Ohkitani [57]: Singularity; no.
11. Grauer, Marliani and Germaschewski [58]: using an adaptive mesh refinement of the Bell and Marcus initial condition [46] with 2048^3 mesh points, they achieved an amplification factor of vorticity of 21. Singularity; yes.
12. Hou and Li [59]: A $1536 \times 1024 \times 3072$ pseudo-spectral calculation agreed with Kerr [48] until the final stage and then the growth slowed; the vorticity grew no faster than double-exponential in time. Singularity; no.
13. Germaschewski and Grauer (2001, unpublished): revisited the Boratav-Pelz simulations but observed strong vortex flattening that halted singular growth. This is consistent with the results of Hou and Li [59]. Singularity; no.
14. Orlandi and Carnevale [60]: using Lamb dipoles as initial conditions, they performed a 1024^3 finite difference calculation with two symmetry planes. They found a period of rapid growth of vorticity consistent with $\|\boldsymbol{\omega}\|_{L^\infty(\Omega)} \sim (T-t)^{-1}$: Singularity; yes.

The interested reader may wish to consult the other articles in this volume written by Hou [61], Bustamente and Kerr [62] and Grauer [63] which contain more references on this topic.

3.3. Results on the direction of vorticity

The yes/no aspect of the results in Section 3.2 is deceptive because the list may have hidden the fact that while a result may have been "no" the vorticity growth may nevertheless have been very strong. It is easy to overlook the directional mechanisms that induce strong early growth even if that growth slows during the final stage. Thus it is important to consider the direction of vorticity growth in its own right [64]. The reader is referred to the companion article in this volume by Constantin [65].

The pioneering paper by Constantin, Fefferman and Majda [66] contains a discussion on the idea of how vortex lines may be considered to be "smoothly directed" in a region of their greatest curvature. A digest of their results is the following: consider the three-dimensional Euler equations with smooth localized initial data and assume the solution is smooth on $0 \le t < T$. The velocity field defines particle trajectories $\boldsymbol{X}(\boldsymbol{x}_0, t)$ that satisfy

$$\frac{\mathrm{D}\boldsymbol{X}}{\mathrm{D}t} = \boldsymbol{u}(\boldsymbol{X}, t), \tag{13}$$

where $\boldsymbol{X}(\boldsymbol{x}_0, 0) = \boldsymbol{x}_0$. The image $\boldsymbol{W}_t$ of a set $\boldsymbol{W}_0$ is given by $\boldsymbol{W}_t = \boldsymbol{X}(\boldsymbol{W}_0, t)$. Then the set $\boldsymbol{W}_0$ is said to be *smoothly directed* if there exists a length $\rho > 0$ and a ball $0 < r < \frac{1}{2}\rho$ such that the following conditions are satisfied: (i) $\hat{\boldsymbol{\omega}}(\cdot, t)$ has a Lipschitz extension to the ball $B_{4\rho}$ of radius 4ρ centred at $\boldsymbol{X}(\boldsymbol{x}_0, t)$; (ii) if the velocity is finite in a ball $B_{4\rho}$; (iii) if

$$\lim_{t\to T} \sup_{W_0} \int_0^t \|\nabla\hat{\boldsymbol{\omega}}(\cdot, \tau)\|^2_{L^\infty(B_{4\rho})} \mathrm{d}\tau < \infty. \tag{14}$$

One needs a chosen neighbourhood that captures large and growing vorticity which does not overlap with another similar region. Under these circumstances, there can be no singularity at time T. Cordoba and Fefferman [67] have weakened condition (ii) in the case of vortex tubes to

$$\int_0^T \|\boldsymbol{u}(\cdot, s)\|_{L^\infty(\Omega)} \mathrm{d}s < \infty. \tag{15}$$

A result a decade later by Deng, Hou and Yu [68,69] follows in the same spirit; they take the arc length $L(t)$ of a vortex line L_t with $\hat{\boldsymbol{n}}$ the unit normal and κ the curvature. Let $0 < B \le 1 - A$, and C_0 be a positive constant with $M(t)$ defined as

$$M(t) \equiv \max\left(\|\nabla\cdot\hat{\boldsymbol{\omega}}\|_{L^\infty(L_t)}, \|\kappa\|_{L^\infty(L_t)}\right). \tag{16}$$

They prove that there will be no blow-up at time T if

$$U_{\hat{\omega}}(t) + U_{\hat{n}}(t) \lesssim (T-t)^{-A}, \tag{17}$$

$$M(t)L(t) \le C_0, \tag{18}$$

$$L(t) \gtrsim (T-t)^{B}. \tag{19}$$

$U_{\hat{\omega}}(t)$ is the maximum value of the tangential velocity of the difference between any two points x and y on the vortex line length L_t; likewise for $U_{\hat{n}}(t)$ with respect to the normal velocity.

4. The pressure Hessian

4.1. Ertel's Theorem and its consequences

The traditional view in fluid mechanics has taken the velocity vector field $\boldsymbol{u}$ as the dominant variable with the pressure p considered as an auxiliary. Given that there exists no evolution equation for p, which must be determined from the elliptic equation (3), there is much to be said for this philosophy. Following Leray, this is normally put into practice in Navier–Stokes and Euler analysis by projection onto divergence-free vector fields, thus covertly hiding the pressure. An alternative route is to avoid this projection process and make a virtue of openly keeping the pressure in the calculation. The key to this route is to use what is generally called Ertel's theorem, which is stated as the following formal result [71]:

Theorem 2. *If $\boldsymbol{\omega}$ satisfies the three-dimensional incompressible Euler equations then any arbitrary differentiable μ satisfies*

$$\frac{\mathrm{D}}{\mathrm{D}t}(\boldsymbol{\omega}\cdot\nabla\mu) = \boldsymbol{\omega}\cdot\nabla\left(\frac{\mathrm{D}\mu}{\mathrm{D}t}\right). \tag{20}$$

The proof is a simple exercise: consider $\boldsymbol{\omega}\cdot\nabla\mu \equiv \omega_i\mu_{,i}$

$$\begin{aligned}\frac{\mathrm{D}}{\mathrm{D}t}(\omega_i\mu_{,i}) &= \frac{\mathrm{D}\omega_i}{\mathrm{D}t}\mu_{,i} + \omega_i\left\{\left(\frac{\mathrm{D}\mu}{\mathrm{D}t}\right)_{,i} - u_{k,i}\mu_{,k}\right\}\\ &= \omega_i\left(\frac{\mathrm{D}\mu}{\mathrm{D}t}\right)_{,i} + \{\omega_j u_{i,j}\mu_{,i} - \omega_i u_{k,i}\mu_{,k}\}.\end{aligned}$$

The last term is zero under summation. Another way of expressing this result is that $\mathrm{D}/\mathrm{D}t$ and $\boldsymbol{\omega}\cdot\nabla$ commute

$$\left[\frac{\mathrm{D}}{\mathrm{D}t}, \boldsymbol{\omega}\cdot\nabla\right] = 0. \tag{21}$$

In Lie-derivative form this means that $\boldsymbol{\omega}\cdot\nabla(t) = \boldsymbol{\omega}\cdot\nabla(0)$ is a Lagrangian invariant and is "frozen in".

In geophysical fluid dynamics, if μ is chosen as the density ρ in a Boussinesq fluid then

$$\frac{\mathrm{D}\rho}{\mathrm{D}t} = 0 \tag{22}$$

implies that $\boldsymbol{\omega}\cdot\nabla\rho$ (potential vorticity) is a constant of the motion [70]. Credit is normally given to Ertel [71] although the general result has been known for much longer [72–74]. Both Klainerman [75] and Ohkitani [76,77] used Theorem 2 in the following way. The choice of $\mu = u_i$ gives a relation for the vortex stretching vector

$$\frac{\mathrm{D}(\boldsymbol{\omega}\cdot\nabla\boldsymbol{u})}{\mathrm{D}t} = \boldsymbol{\omega}\cdot\nabla\left(\frac{\mathrm{D}\boldsymbol{u}}{\mathrm{D}t}\right) = -P\boldsymbol{\omega}, \tag{23}$$

where P is the Hessian matrix of the pressure

$$P = \{p_{,ij}\} = \left\{\frac{\partial^2 p}{\partial x_i\partial x_j}\right\}. \tag{24}$$

This result illustrates the relative merits or demerits of cancelling non-linearity of $O(|\boldsymbol{\omega}||\nabla\boldsymbol{u}|^2)$ while being forced to include the Hessian of the pressure.

4.2. Restricted Euler equations: Modelling the pressure Hessian

The results of the previous subsection have shown that if the pressure field is to remain in the calculation then it is important to understand its Hessian matrix. Because there are numerical difficulties in accurately computing this matrix there have been a variety of attempts at modelling it. In effect, this produces restricted versions of the Euler equations. Consider the gradient matrix $M_{ij} = u_{i,j}$ which satisfies the matrix Riccati equation

$$\frac{\mathrm{D}M}{\mathrm{D}t} + M^2 + P = 0, \tag{25}$$

$$\mathrm{Tr}\,P = -\mathrm{Tr}\,(M^2), \tag{26}$$

where Eq. (26) has its origins in the divergence-free condition $\mathrm{Tr}\,M = 0$ and is an economical way of writing $\Delta p = -u_{i,j}u_{j,i}$. Several attempts have been made to model the Lagrangian-averaged pressure Hessian by introducing a constitutive closure — see [78] for a summary. The idea goes back to Léorat [79], Vieillefosse [80], Novikov [81] and Cantwell [82]. The Eulerian pressure Hessian P is generally assumed to be isotropic

$$P = -\frac{1}{3}I\,\mathrm{Tr}\,(M^2), \quad \mathrm{Tr}\,I = 3, \tag{27}$$

which results in the "restricted Euler equations". There is a also a variety of literature on modelling the velocity gradient matrix [83–86]. The elliptic pressure constraint given in (3), re-expressed as $-\mathrm{Tr}\,P = \mathrm{Tr}\,(S^2) - \frac{1}{2}\omega^2$, is concerned solely with the diagonal elements of P, whereas in computations its off-diagonal elements turn out to be important.

An different attempt at modelling the effect of the Hessian has been made by Constantin who derived the "distorted Euler equations" [87]. The Euler equations for the gradient composed with the Lagrangian path map $\boldsymbol{a} \mapsto \boldsymbol{X}(\boldsymbol{a}, t)$, $N = M\circ\boldsymbol{X}$ are rewritten in Lagrangian form as

$$\frac{\partial N}{\partial t} + N^2 + Q(\boldsymbol{x}, t)\mathrm{Tr}(N^2) = 0, \tag{28}$$

$$Q_{ij} = R_iR_j\circ\boldsymbol{X}, \qquad R_i = (-\Delta)^{-1/2}\frac{\partial}{\partial x_i}, \tag{29}$$

where R_i is the Riesz transform and $\boldsymbol{X}$ represents the Lagrangian path-map $\boldsymbol{a} \mapsto \boldsymbol{X}(\boldsymbol{a}, t)$. The distorted equations arise through replacing $Q_{ij}(t)$ with $Q_{ij}(0)$, solutions of which have been proved to blow up [87]. Other models of interest include the tetrad model of Chertkov, Pumir and Shraiman [88] which has recently been developed by Chevillard and Meneveau [89]. More ideas regarding the modelling of the pressure Hessian through a transformation from Eulerian to Lagrangian coordinates using a Lagrangian flow map have recently been discussed in [78].

5. A formulation in quaternions

The material of Section 3.3 has been devoted to the issue of the directional growth of vorticity. Ultimately, the mechanisms that guide this growth will determine whether the Euler equations develop a finite-time singularity and so alternative ways of formulating this problem may be of value. It turns out that Hamilton's quaternions are useful not only for this purpose but are also ideal for understanding how fluid particles rotate within their trajectories. Before moving on to more technical aspects of quaternions some motivation is in order to explain why their introduction into Euler analysis is natural.

Firstly, based on the unit vector of vorticity $\hat{\boldsymbol{\omega}}$, let us define the respective scalar and 3-vector variables designated as α and $\boldsymbol{\chi}$

$$\alpha = \hat{\boldsymbol{\omega}} \cdot S\hat{\boldsymbol{\omega}}, \qquad \boldsymbol{\chi} = \hat{\boldsymbol{\omega}} \times S\hat{\boldsymbol{\omega}}. \tag{30}$$

These respectively represent the rates of growth and swing of the vorticity. Then the vortex stretching vector $S\boldsymbol{\omega}$ can be decomposed into components parallel and perpendicular to $\boldsymbol{\omega}$

$$S\boldsymbol{\omega} = \alpha\boldsymbol{\omega} + \boldsymbol{\chi} \times \boldsymbol{\omega}, \tag{31}$$

from which it is trivial to show that $\omega = |\boldsymbol{\omega}|$ and $\hat{\boldsymbol{\omega}}$ satisfy

$$\frac{\mathrm{D}\omega}{\mathrm{D}t} = \alpha\omega, \qquad \frac{\mathrm{D}\hat{\boldsymbol{\omega}}}{\mathrm{D}t} = \boldsymbol{\chi} \times \hat{\boldsymbol{\omega}}. \tag{32}$$

It is clear that in the evolution of $\alpha(\boldsymbol{x}, t)$ and $\boldsymbol{\chi}(\boldsymbol{x}, t)$ lies the key to the growth and direction of vorticity. Given that α and $\boldsymbol{\chi}$, by definition, contain $S\boldsymbol{\omega}$, it is also clear from (23) that material differentiation of them will introduce the pressure Hessian P into the problem and thus the advantages and disadvantages discussed in Section 4 regarding its use come into play. Combining α and $\boldsymbol{\chi}$ into a 4-vector quaternion is an obvious first step; thereafter we wish to exploit the elegant algebraic properties that quaternions possess.

The second area where quaternions have an application lies in the recent experimental advances that have made in the detection of the trajectories of tracer and other particles in fluid flows [90–99]. The curvature of their paths can be used to extract statistical information about velocity gradients from a single trajectory. Fluid particles not only take complicated trajectories but they also rotate in motion. Recent work has shown that Hamilton's quaternions are applicable to this type of problem [78,100–103]. In his lifetime Hamilton's ideas did not meet with the approval of his contemporaries [104–106] but in the context of modern-day problems the crucial property that quaternions possess – that they represent a composition of rotations – has made them the technical foundation of modern inertial guidance systems in the aerospace industry where tracking the paths and the orientation of satellites and aircraft is critical [107]. The graphics community also uses them to control the orientation of tumbling objects in computer animations [108] because they avoid the difficulties incurred at the poles when Euler angles are used [108–110]. When quaternions are applicable to a problem it is usually evidence that geometrical structures are dominant. This aspect of the Euler equations has been long been debated [64,103,111–114]. Given the available equations for the evolution of the vorticity $\boldsymbol{\omega}$, the strain matrix S, and the Hessian matrix P, a pertinent question to ask is whether this is enough information to make a satisfactory formulation of this problem.

In the first of future subsections a general class of Lagrangian evolution equations will be considered of which Euler is the most important member. Then the properties of quaternions and their association with rigid body dynamics is summarized in Section 5.2 and applied in Section 5.3 to the description the flight and rotation of fluid particles. In this it will be seen how the pressure Hessian is the key factor in driving the system. Sections 5.4 and 5.5 are devoted to some of the properties of the Euler equations themselves.

5.1. *A class of Lagrangian evolution equations*

Suppose $\boldsymbol{w}$ is a contravariant vector quantity attached to a particle following a flow along the characteristic paths $d\boldsymbol{x}/dt = \boldsymbol{u}$ of a velocity field $\boldsymbol{u}(\boldsymbol{x}, t)$. Now consider the formal Lagrangian flow equation [78]

$$\frac{\mathrm{D}\boldsymbol{w}}{\mathrm{D}t} = \boldsymbol{a}(\boldsymbol{x}, t), \tag{33}$$

where the material derivative is given by (2). Let us also suppose that $\boldsymbol{a}$ itself is formally differentiable

$$\frac{\mathrm{D}\boldsymbol{a}}{\mathrm{D}t} = \boldsymbol{b}(\boldsymbol{x}, t), \tag{34}$$

where $\boldsymbol{b}(\boldsymbol{x}, t)$ is known. Together (2), (33) and (34) define a quartet of 3-vectors

$$\{\boldsymbol{u}, \boldsymbol{w}, \boldsymbol{a}, \boldsymbol{b}\}. \tag{35}$$

For a passive particle, $\boldsymbol{u}$ and $\boldsymbol{w}$ are independent vectors but for the three-dimensional Euler equations $\boldsymbol{u}$ and $\boldsymbol{w} \equiv \boldsymbol{\omega}$ are tied by the fact that $\boldsymbol{\omega} = \mathrm{curl}\,\boldsymbol{u}$. The quartet in (35) is now

$$\{\boldsymbol{u}, \boldsymbol{w}, \boldsymbol{a}, \boldsymbol{b}\} = \{\boldsymbol{u}, \boldsymbol{\omega}, S\boldsymbol{\omega}, -P\boldsymbol{\omega}\}, \tag{36}$$

where P is the pressure Hessian discussed in Section 4. This is not the whole story because the divergence-free condition means that P, S and $\boldsymbol{\omega}$ are not independent of each other because of the elliptic pressure constraint

$$-\mathrm{Tr}\,P = \mathrm{Tr}\left(S^2\right) - \frac{1}{2}\omega^2. \tag{37}$$

Another example that could be cast into this format are the equations of ideal MHD in Elsasser form (see [78,100,101] although the existence of two material derivatives requires some generalization.

In Section 5.3 it will be shown how the quartet in (35), based upon the pair of Lagrangian evolution equations (33) and (34), can determine the evolution of an ortho-normal frame for a fluid particle in a trajectory. In graphics problems the usual practice is to consider the Frenet-frame of a trajectory. This consists of the unit tangent vector, a normal and a bi-normal [108]. In navigational language, this represents the corkscrew-like pitch, yaw and roll of the motion. In turn, the tangent vector and normals are related to the curvature and torsion. While the Frenet-frame describes the path, it ignores the dynamics that generates the motion. Here we will discuss another ortho-normal frame associated with the motion of each Lagrangian fluid particle, designated the *quaternion-frame*. This may be envisaged as moving with the Lagrangian particles, but their evolution derives from the Eulerian equations of motion.

5.2. Quaternions and rigid body dynamics

Rotations in rigid body mechanics have given rise to a rich and longstanding literature in which Whittaker's book is a classic example [110]. This gives explicit formulae relating the Euler angles to the Euler parameters and Cayley–Klein parameters of a rotation. Quaternions are not only much more efficient but they also circumvent the messy inter-relations that are unavoidable when Euler angle formulae are involved [105, 110].

In terms of any scalar p and any 3-vector $\boldsymbol{q}$, the quaternion $\mathfrak{q} = [p, \boldsymbol{q}]$ is defined as

$$\mathfrak{q} = [p, \boldsymbol{q}] = pI - \sum_{i=1}^{3} q_i \sigma_i, \tag{38}$$

in which Gothic fonts denote quaternions (see [78,100]). The three Pauli spin matrices σ_i are defined by

$$\sigma_1 = \begin{pmatrix} 0 & i \\ i & 0 \end{pmatrix} \quad \sigma_2 = \begin{pmatrix} 0 & 1 \\ -1 & 0 \end{pmatrix} \quad \sigma_3 = \begin{pmatrix} i & 0 \\ 0 & -i \end{pmatrix} \tag{39}$$

and I is the 2×2 unit matrix. The relations between the Pauli matrices $\sigma_i \sigma_j = -\delta_{ij} I - \epsilon_{ijk} \sigma_k$ then give a non-commutative multiplication rule

$$\mathfrak{q}_1 \circledast \mathfrak{q}_2 = [p_1 p_2 - \boldsymbol{q}_1 \cdot \boldsymbol{q}_2, p_1 \boldsymbol{q}_2 + p_2 \boldsymbol{q}_1 + \boldsymbol{q}_1 \times \boldsymbol{q}_2]. \tag{40}$$

It is not difficult to demonstrate that they are associative.

Let $\hat{\mathfrak{p}} = [p, \boldsymbol{q}]$ be a unit quaternion with inverse $\hat{\mathfrak{p}}^* = [p, -\boldsymbol{q}]$: this requires $\hat{\mathfrak{p}} \circledast \hat{\mathfrak{p}}^* = [p^2 + q^2, 0] = [1, 0]$. For a pure quaternion $\mathfrak{r} = [0, \boldsymbol{r}]$ there exists a transformation

$$\mathfrak{r} = [0, \boldsymbol{r}] \mapsto \mathfrak{R} = [0, \boldsymbol{R}] \tag{41}$$

that can explicitly be written as

$$\mathfrak{R} = \hat{\mathfrak{p}} \circledast \mathfrak{r} \circledast \hat{\mathfrak{p}}^* = [0, (p^2 - q^2)\boldsymbol{r} + 2p(\boldsymbol{q} \times \boldsymbol{r}) + 2\boldsymbol{q}(\boldsymbol{r} \cdot \boldsymbol{q})]. \tag{42}$$

Choosing p and $\boldsymbol{q}$ such that $\hat{\mathfrak{p}} = \pm[\cos \frac{1}{2}\theta, \hat{\boldsymbol{n}} \sin \frac{1}{2}\theta]$, where $\hat{\boldsymbol{n}}$ is the unit normal to $\boldsymbol{r}$, we find that

$$\begin{aligned} \mathfrak{R} = \hat{\mathfrak{p}} \circledast \mathfrak{r} \circledast \hat{\mathfrak{p}}^* &= [0, \boldsymbol{r} \cos\theta + (\hat{\boldsymbol{n}} \times \boldsymbol{r}) \sin\theta] \\ &\equiv O(\theta, \hat{\boldsymbol{n}})\boldsymbol{r}. \end{aligned} \tag{43}$$

Eq. (43) is the *Euler–Rodrigues formula* for the rotation $O(\theta, \hat{\boldsymbol{n}})$ by an angle θ of the 3-vector $\boldsymbol{r}$ about its normal $\hat{\boldsymbol{n}}$ and $(\theta, \hat{\boldsymbol{n}})$ are called the Euler parameters. The elements of the unit quaternion $\hat{\mathfrak{p}}$ are the Cayley–Klein parameters which are related to the Euler angles [110], and form a representation of the Lie group $SU(2)$. When $\hat{\mathfrak{p}}$ is time-dependent, the Euler–Rodrigues formula in (43) can be rewritten as

$$\mathfrak{r} = \hat{\mathfrak{p}}^* \circledast \mathfrak{R}(t) \circledast \hat{\mathfrak{p}} \tag{44}$$

and thus the time derivative $\dot{\mathfrak{R}}$ is given by

$$\dot{\mathfrak{R}}(t) = (\dot{\hat{\mathfrak{p}}} \circledast \hat{\mathfrak{p}}^*) \circledast \mathfrak{R} - ((\dot{\hat{\mathfrak{p}}} \circledast \hat{\mathfrak{p}}^*) \circledast \mathfrak{R})^*, \tag{45}$$

where we have used the fact that $\mathfrak{R}^* = -\mathfrak{R}$. Because $\hat{\mathfrak{p}} = [p, \boldsymbol{q}]$ is of unit length, and thus $p\dot{p} + q\dot{q} = 0$, this means that $\dot{\hat{\mathfrak{p}}} \circledast \hat{\mathfrak{p}}^* = [0, \frac{1}{2}\boldsymbol{\Omega}_0(t)]$ which is also a pure quaternion. The 3-vector entry in this defines the angular frequency $\boldsymbol{\Omega}_0(t)$ as $\boldsymbol{\Omega}_0 = 2(-\dot{p}\boldsymbol{q} + \dot{\boldsymbol{q}}p - \dot{\boldsymbol{q}} \times \boldsymbol{q})$ thereby giving the well-known formula for the rotation of a rigid body

$$\dot{\boldsymbol{R}} = \boldsymbol{\Omega}_0 \times \boldsymbol{R}. \tag{46}$$

For a Lagrangian particle, the equivalent of $\boldsymbol{\Omega}_0$ is the Darboux vector $\boldsymbol{\mathcal{D}}_a$ in Theorem 3 of Section 5.3.

5.3. An ortho-normal frame and particle trajectories

Having set the scene in Section 5.2 by describing some of the essential properties of quaternions, it is now time to apply them to the Lagrangian relation (33) between the two vectors $\boldsymbol{w}$ and $\boldsymbol{a}$. Through the multiplication rule in (40) quaternions appear in the decomposition of the 3-vector $\boldsymbol{a}$ into parts parallel and perpendicular to $\boldsymbol{w}$, which is expressed as

$$\boldsymbol{a} = \alpha_a \boldsymbol{w} + \boldsymbol{\chi}_a \times \boldsymbol{w} = [\alpha_a, \boldsymbol{\chi}_a] \circledast [0, \boldsymbol{w}]. \tag{47}$$

The scalar α_a and 3-vector $\boldsymbol{\chi}_a$ in (47) are defined as

$$\alpha_a = w^{-1}(\hat{\boldsymbol{w}} \cdot \boldsymbol{a}), \quad \boldsymbol{\chi}_a = w^{-1}(\hat{\boldsymbol{w}} \times \boldsymbol{a}). \tag{48}$$

It is now easily seen that α_a is the growth rate of the scalar magnitude ($w = |\boldsymbol{w}|$) which obeys

$$\frac{\mathrm{D}w}{\mathrm{D}t} = \alpha_a w, \tag{49}$$

while $\boldsymbol{\chi}_a$, the swing rate of the unit tangent vector $\hat{\boldsymbol{w}} = \boldsymbol{w}w^{-1}$, satisfies

$$\frac{\mathrm{D}\hat{\boldsymbol{w}}}{\mathrm{D}t} = \boldsymbol{\chi}_a \times \hat{\boldsymbol{w}}. \tag{50}$$

Now define the two quaternions

$$\mathfrak{q}_a = [\alpha_a, \boldsymbol{\chi}_a], \qquad \mathfrak{w} = [0, \boldsymbol{w}], \tag{51}$$

where $\mathfrak{w}$ is a pure quaternion. Then (33) can automatically be rewritten equivalently in the quaternion form

$$\frac{\mathrm{D}\mathfrak{w}}{\mathrm{D}t} = \mathfrak{q}_a \circledast \mathfrak{w}. \tag{52}$$

Moreover, if $\boldsymbol{a}$ is differentiable in the Lagrangian sense so that its material derivative is $\boldsymbol{b}$, as in (34) then another quaternion $\mathfrak{q}_b$ can be defined, based on the variables

$$\alpha_b = w^{-1}(\hat{\boldsymbol{w}} \cdot \boldsymbol{b}), \qquad \boldsymbol{\chi}_b = w^{-1}(\hat{\boldsymbol{w}} \times \boldsymbol{b}), \tag{53}$$

where

$$\mathfrak{q}_b = [\alpha_b, \boldsymbol{\chi}_b]. \tag{54}$$

Clearly there exists a similar decomposition for $\boldsymbol{b}$ as that for $\boldsymbol{a}$ as in (47)

$$\frac{\mathrm{D}^2\mathfrak{w}}{\mathrm{D}t^2} = [0, \boldsymbol{b}] = [0, \alpha_b \boldsymbol{w} + \boldsymbol{\chi}_b \times \boldsymbol{w}] = \mathfrak{q}_b \circledast \mathfrak{w}. \tag{55}$$

Using the associativity property, compatibility of (55) and (52) implies that ($w = |\boldsymbol{w}| \neq 0$)

$$\left(\frac{\mathrm{D}\mathfrak{q}_a}{\mathrm{D}t} + \mathfrak{q}_a \circledast \mathfrak{q}_a - \mathfrak{q}_b\right) \circledast \mathfrak{w} = 0, \tag{56}$$

which establishes a *Riccati relation* between $\mathfrak{q}_a$ and $\mathfrak{q}_b$

$$\frac{\mathrm{D}\mathfrak{q}_a}{\mathrm{D}t} + \mathfrak{q}_a \circledast \mathfrak{q}_a = \mathfrak{q}_b, \tag{57}$$

whose components yield

$$\frac{\mathrm{D}}{\mathrm{D}t}[\alpha_a, \boldsymbol{\chi}_a] + [\alpha_a^2 - \chi_a^2, 2\alpha_a \boldsymbol{\chi}_a] = [\alpha_b, \chi_b]. \tag{58}$$

These lead to a general theorem on the nature of the dynamics of the ortho-normal frame (see Fig. 1):

Theorem 3 (*[78,100]*). *The ortho-normal quaternion-frame* $(\hat{\boldsymbol{w}}, \hat{\boldsymbol{\chi}}_a, \hat{\boldsymbol{w}} \times \hat{\boldsymbol{\chi}}_a) \in SO(3)$ *has Lagrangian time derivatives expressed as* ($w \neq 0$)

$$\frac{\mathrm{D}\hat{\boldsymbol{w}}}{\mathrm{D}t} = \boldsymbol{\mathcal{D}}_a \times \hat{\boldsymbol{w}}, \tag{59}$$

$$\frac{\mathrm{D}(\hat{\boldsymbol{w}} \times \hat{\boldsymbol{\chi}}_a)}{\mathrm{D}t} = \boldsymbol{\mathcal{D}}_a \times (\hat{\boldsymbol{w}} \times \hat{\boldsymbol{\chi}}_a), \tag{60}$$

$$\frac{\mathrm{D}\hat{\boldsymbol{\chi}}_a}{\mathrm{D}t} = \boldsymbol{\mathcal{D}}_a \times \hat{\boldsymbol{\chi}}_a. \tag{61}$$

The Darboux angular velocity vector $\boldsymbol{\mathcal{D}}_a$ *is defined as*

$$\boldsymbol{\mathcal{D}}_a = \boldsymbol{\chi}_a + \frac{c_b}{\chi_a}\hat{\boldsymbol{w}}, \quad c_b = \hat{\boldsymbol{w}} \cdot (\hat{\boldsymbol{\chi}}_a \times \boldsymbol{\chi}_b). \tag{62}$$

Remark 1. The proof of Theorem 3 is simple and can be found in [78,100]. The Darboux vector $\boldsymbol{\mathcal{D}}_a$ sits in a two-dimensional plane and is driven by the vector $\boldsymbol{b}$ which itself sits in c_b in (62). The analogy with rigid body rotation expressed in (46) is clear.

Remark 2. This theorem is much more general than might be initially apparent. It provides an elegant and simple means of constructing the dynamic equations for an ortho-normal frame for any system driven by a field $\boldsymbol{b}$. An example of this is the construction of a frame for the Kepler system which is illustrated in [114].

5.4. Relation to the Euler equations

For the three-dimensional Euler equations themselves the scalar and vector variables $\alpha, \boldsymbol{\chi}$ have already been defined in (30) as the scalar and vector products between $\boldsymbol{\omega}$ and $S\boldsymbol{\omega}$. The variables $\alpha_p, \boldsymbol{\chi}_p$ corresponding (53) (with a change of sign) are defined in the same manner [101,102]

$$\alpha_p = \hat{\boldsymbol{\omega}} \cdot P\hat{\boldsymbol{\omega}}, \qquad \boldsymbol{\chi}_p = \hat{\boldsymbol{\omega}} \times P\hat{\boldsymbol{\omega}}, \tag{63}$$

which avoids the null points that arise in the definition in (48) and (53). The definitions of $\alpha, \alpha_p, \boldsymbol{\chi}, \boldsymbol{\chi}_p$ were first written down in [103]. In fact, α and α_p are Rayleigh quotient estimates for eigenvalues of S and P respectively although they are only exact eigenvalues when $\boldsymbol{\omega}$ aligns with one of their eigenvectors. Constantin [64] has a Biot–Savart formula for α. These variables form natural tetrads associated with $[0, \boldsymbol{\omega}]$

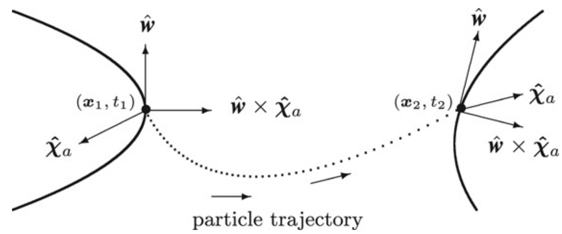

Fig. 1. Three unit vectors $[\hat{\boldsymbol{w}}, \hat{\boldsymbol{\chi}}, \hat{\boldsymbol{w}} \times \hat{\boldsymbol{\chi}}]$ form an ortho-normal coordinate system on a characteristic curve $\mathrm{d}\boldsymbol{x}/\mathrm{d}s = \boldsymbol{u}$. The two curves are drawn at times t_1 and t_2: the dotted curve represents the particle trajectory.

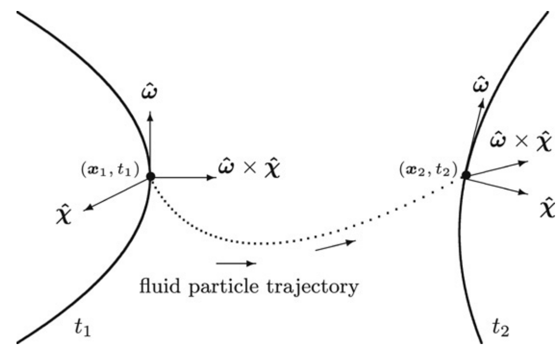

Fig. 2. Vortex lines (solid) on which sit an ortho-normal frame $\hat{\boldsymbol{\omega}}, \hat{\boldsymbol{\chi}}, \hat{\boldsymbol{\omega}} \times \hat{\boldsymbol{\chi}}$ for the Euler equations. The two curves are drawn at times t_1 and t_2: the dotted curve represents a fluid particle trajectory.

$$\mathfrak{q} = [\alpha, \boldsymbol{\chi}], \qquad -\mathfrak{q}_b = \mathfrak{q}_p = \left[\alpha_p, \boldsymbol{\chi}_p\right]. \tag{64}$$

Thus it is the pressure Hessian P that lies in $\mathfrak{q}_p$ and controls the particle trajectories through

$$\frac{\mathrm{D}\mathfrak{q}}{\mathrm{D}t} + \mathfrak{q} \circledast \mathfrak{q} + \mathfrak{q}_p = 0. \tag{65}$$

Theorem 3 furnishes us with an equivalent set of equations for the ortho-normal frame $(\hat{\boldsymbol{\omega}}, \hat{\boldsymbol{\chi}}, \hat{\boldsymbol{\omega}} \times \hat{\boldsymbol{\chi}})$ of a fluid particle through (62) where

$$c_p = -\hat{\boldsymbol{\omega}} \cdot (\hat{\boldsymbol{\chi}} \times \boldsymbol{\chi}_p). \tag{66}$$

The dynamics of the ortho-normal frame could be seen as a competition between S and P with the divergence-free constraint (37) applied.

5.5. The Frenet frame

Modulo a rotation around the unit tangent vector $\hat{\boldsymbol{\omega}}$ of Fig. 2, with $\hat{\boldsymbol{\chi}}$ as the unit bi-normal $\hat{\boldsymbol{b}}$ and $\hat{\boldsymbol{\omega}} \times \hat{\boldsymbol{\chi}}$ as the unit principal normal $\hat{\boldsymbol{n}}$ to the vortex line, the matrix F can be formed

$$F = \left(\hat{\boldsymbol{\omega}}^T, (\hat{\boldsymbol{\omega}} \times \hat{\boldsymbol{\chi}})^T, \hat{\boldsymbol{\chi}}^T\right), \tag{67}$$

and (59)–(61) can be re-written as

$$\frac{DF}{\mathrm{D}t} = AF, \quad A = \begin{pmatrix} 0 & -\chi & 0 \\ \chi & 0 & c_p\chi^{-1} \\ 0 & -c_p\chi^{-1} & 0 \end{pmatrix}. \tag{68}$$

For a space curve parameterized by arc-length s, then the Frenet equations relating $\mathrm{d}F/\mathrm{d}s$ to the curvature κ and the torsion τ of the vortex line curve are

$$\frac{\mathrm{d}F}{\mathrm{d}s} = NF, \quad \text{where } N = \begin{pmatrix} 0 & \kappa & 0 \\ -\kappa & 0 & \tau \\ 0 & -\tau & 0 \end{pmatrix}. \tag{69}$$

It is now possible to relate the t and s derivatives of F given in (68) and (69). At any time t the integral curves of the vorticity vector field define a space-curve through each point $\boldsymbol{x}$. The arc-length derivative is defined by

$$\frac{\mathrm{d}}{\mathrm{d}s} = \hat{\boldsymbol{\omega}} \cdot \nabla. \tag{70}$$

The evolution of the curvature κ and torsion τ of a vortex line may be obtained from Ertel's theorem in (21), expressed as the commutation of operators

$$\left[\frac{\mathrm{d}}{\mathrm{d}s}, \frac{\mathrm{D}}{\mathrm{D}t}\right] = \alpha \frac{\mathrm{d}}{\mathrm{d}s}. \tag{71}$$

Applying this to F and using the relations (68) and (69) establishes the following consistency relation on the matrices N and A

$$\frac{\mathrm{D}N}{\mathrm{D}t} - \alpha N = \frac{\mathrm{d}A}{\mathrm{d}s} + [A, N] \tag{72}$$

which relates the evolution of the curvature κ and the torsion τ to α, χ and c_p defined in (30) and (62).

6. Final remarks

It is clear that despite past endeavours there is still a very long way to go before we can say that there exists a clear mathematical understanding of the behaviour of solutions of the incompressible three-dimensional Euler equations. While weak solutions in the conventional sense of Leray are not known to exist, certain very special weak solutions have been found, such as those constructed by Brenier [115] and Shnirelman [116]. These are obtained by relaxing the variational problem and are not the same as weak solutions of the initial value problem for the Euler equations themselves.

The existence or non-existence of singularities is still an open problem. The numerical results of Hou and Li [59], which have focused anew on Kerr's numerical calculations performed fourteen years ago [48], suggest that a new generation of numerical experiments may be needed to look more carefully at not only the amplitude but also the direction of vorticity at high amplitudes. Even with a combination of analysis, as in [59,66–69], and with potentially much greater computing power, we may still have to wait some time until this matter is settled decisively. Much of the literature in modern mechanics has stressed that the three-dimensional Euler equations have inherent geometrical properties [11,64,66,111–113]. It is thus possible that the open problem of the regularity of solutions may become clearer after using a combination of geometrical and topological fluid mechanics [10–15] in combination with analysis and large-scale numerical computations. However, it is not clear what theorem might emerge from these considerations. Until then, the singularity problem will remain as one of the great challenges in modern applied mathematics.

A further area of endeavour has lain in the modelling of the pressure Hessian and the velocity gradient matrix. The traditional view in fluid mechanics holds that the pressure should be treated as an auxiliary variable. The alternative is to treat the Hessian P on an equal footing with the strain matrix S. Out of necessity this is certainly the case when quaternions are used to describe the problem. The elliptic equation for the pressure

$$-\Delta p = -\mathrm{Tr}\, P = \mathrm{Tr}\left(S^2\right) - \frac{1}{2}\omega^2, \tag{73}$$

is by no means fully understood and *locally* holds the key to the formation of vortical structures through the sign of $\mathrm{Tr}\, P$. In this relation, which is often thought of as a constraint, may lie a deeper knowledge of the geometry of both the Euler and Navier–Stokes equations. In turn, this may lead to a better understanding of the role of the pressure. Eq. (73) certainly plays a role in three-dimensional Navier–Stokes turbulence calculations in which the vortical topology has the classic signature of what are called "thin sets", where the vorticity concentrates into quasi-two-dimensional vortex sheets which later have a tendency to roll up into quasi-one-dimensional tubes. These tubes have a complicated topology and a finite lifetime, vanishing in one location and reappearing in another [22]. The fact that these thin sets are dynamically favoured may be explained by inherent geometrical properties of the Euler equations but little is known about these features.

Let us end with an analogy: if work on the Euler equations, beginning as a spring of water in the hills 250 years ago, has now become a mature river in full flow, it is probable that it still has far to go before it reaches its distant estuary and ocean. Will the participants at the meeting *Euler 500 years on* in the year 2257 be able to testify that sufficient progress has been made that many of the outstanding problems in this area have been solved?

Acknowledgments

Thanks are due to Uriel Frisch and his collaborators for the excellence of their organization of the meeting *Euler 250 years on*. I would like to thank Claude Bardos, Peter Constantin, Uriel Frisch, Rainer Grauer, Raymond Hide, Darryl Holm, Tom Hou, Bob Kerr, Keith Moffatt, Koji Ohkitani, Ian Roulstone, Trevor Stuart and Edriss Titi for helpful comments and corrections on the material both in this paper and the content of my lecture.

References

[1] Ecclesiasticus 44:1-15, King James Bible (1611), The Oxford Text Archive, http://ota.ahds.ac.uk/.

[2] L. Euler, Principia motus fluidorum, Novi Commentarii Acad. Sci. Petropolitanae 6 (1761) 271–311.

[3] O. Darrigol, Worlds of Flow, Oxford University Press, Oxford, 2007.
[4] V.I. Yudovich, Non-stationary flow of an incompressible liquid, Zh. Vychisl. Mat. Mat. Fiz. 3 (1963) 1032–1066.
[5] P. Constantin, C. Foias, Navier–Stokes Equations, The University of Chicago Press, Chicago, 1988.
[6] A.J. Majda, A.L. Bertozzi, Vorticity and Incompressible Flow, Cambridge University Press, Cambridge, 2001.
[7] L. Woltjer, A theorem on force-free magnetic fields, Proc. Natl. Acad. Sci. 44 (1958) 489–491.
[8] H.K. Moffatt, Magnetic Field Generation in Electrically Conducting Fluids, Cambridge University Press, Cambridge, 1978.
[9] R. Moreau, Magnetohydrodynamics, Kluwer, Dordrecht, 1990.
[10] H.K. Moffatt, The degree of knottedness of tangled vortex lines, J. Fluid Mech. 35 (1969) 117–129.
[11] V.I. Arnold, B.A. Khesin, Topological Methods in Hydrodynamics; Springer Series: Applied Mathematical Sciences, Berlin, 1998.
[12] H.K. Moffatt, Magnetostatic equilibria and analogous Euler flows of arbitrarily complex topology, J. Fluid Mech. 159 (1985) 359–378.
[13] H.K. Moffatt, A. Tsinober (Eds.), Topological Fluid Mechanics: Proceedings of the IUTAM Symposium, Cambridge University Press, 1990.
[14] H.K. Moffatt, A. Tsinober, Helicity in laminar and turbulent flow, Ann. Rev. Fluid Mech. 24 (1992) 281–312.
[15] R.L. Ricca, H.K. Moffatt, The helicity of a knotted vortex filament, in: H.K. Moffatt, G.M. Zaslavsky, P. Compte, M. Tabor (Eds.), Topological Aspects of Fluid Dynamics and Plasmas, Kluwer, Dordrecht, 1992, pp. 235–236.
[16] J.Y. Chemin, Persistance de structures geometriques dans les fluides incompressibles bidimensionnels, Ann. Ec. Norm. Supér. 26 (4) (1993) 1–16.
[17] A. Bertozzi, P. Constantin, Global regularity for vortex patches, Comm. Math. Phys. 152 (1993) 19–28.
[18] J.T. Stuart, Singularities in three-dimensional compressible Euler flows with vorticity, Theoret. Comput. Fluid Dyn. 10 (1998) 385–391.
[19] K. Ohkitani, J.D. Gibbon, Numerical study of singularity formation in a class of Euler and Navier–Stokes flows, Phys. Fluids 12 (2000) 3181–3194.
[20] C.W. Oseen, Exakte Lösungen der hydrodynamischen Differentialgleichungen II, Arkiv für Mat., Astronomi och Fysik 20A (1927) 1.
[21] P. Constantin, The Euler equations and nonlocal conservative Riccati equations, Int. Math. Res. Not. 9 (2000) 455–465.
[22] S. Douady, Y. Couder, M. Brachet, Direct observation of the intermittency of intense vorticity filaments in turbulence, Phys. Rev. Lett. 67 (1991) 983–986.
[23] R.M. Kerr, Higher-order derivative correlations and the alignment of small-scale structures in isotropic numerical turbulence, J. Fluid Mech. 153 (1985) 31–58.
[24] S. Kishiba, K. Ohkitani, S. Kida, Interaction of helical modes in formation of vortical structures in decaying isotropic turbulence, J. Phys. Soc. Japan 64 (1994) 2133–2148.
[25] J.D. Gibbon, D.R. Moore, J.T. Stuart, Exact, infinite energy, blow-up solutions of the three-dimensional Euler equations, Nonlinearity 16 (2003) 1823–1831.
[26] G. Eyink, Dissipative anomalies in singular Euler flows, Physica D 237 (14–17) (2008) 1956–1968.
[27] J.T. Beale, T. Kato, A.J. Majda, Remarks on the breakdown of smooth solutions for the 3D Euler equations, Comm. Math. Phys. 94 (1984) 61–66.
[28] C. Bardos, E. Titi, Euler equations of incompressible ideal fluids, Russian Math. Surveys 62 (3) (2007) 409–451.
[29] A. Ferrari, On the blow-up of solutions of the 3D Euler equations in a bounded domain, Comm. Math. Phys. 155 (1993) 277–294.
[30] H. Kozono, Y. Taniuchi, Limiting case of the Sobolev inequality in BMO, with applications to the Euler equations, Comm. Math. Phys. 214 (2000) 191–200.
[31] G. Ponce, Remarks on a paper by J.T. Beale, T. Kato and A. Majda, Comm. Math. Phys. 98 (1985) 349–353.
[32] D. Chae, Remarks on the blow-up of the Euler equations and the related equations, Comm. Math. Phys. 245 (2003) 539–550.
[33] D. Chae, Local existence and blow-up criterion for the Euler equations in the Besov spaces, Asymptot. Anal. 38 (2004) 339–358.
[34] D. Chae, Remarks on the blow-up criterion of the 3D Euler equations, Nonlinearity 18 (2005) 1021–1029.
[35] D. Chae, On the finite time singularities of the 3D incompressible Euler equations, Comm. Pure Appl. Math. 60 (2007) 597–617.
[36] S. Kida, Three-dimensional periodic flows with high-symmetry, J. Phys. Soc. Japan 54 (1985) 2132–2136.
[37] S. Kida (Ed.), Special issues in memory of Richard Pelz Fluid Dynam. Res. 36 (4–6) (2005).
[38] R.H. Morf, S. Orszag, U. Frisch, Spontaneous singularity in three-dimensional, inviscid incompressible flow, Phys. Rev. Lett. 44 (1980) 572–575.
[39] C. Bardos, S. Benachour, M. Zerner, Analyticité des solutions périodiques de léquation d'Euler en deux dimensions, C. R. Acad. Sci. Paris 282A (1976) 995–998.
[40] C. Bardos, S. Benachour, Domaine d'analyticité des solutions de l'équation d'Euler dans un ouvert de R^n, Ann. Sc. Norm. Super. Pisa, Cl. Sci. IV Ser. 4 (1977) 647–687.
[41] W. Pauls, T. Matsumoto, U. Frisch, J. Bec, Nature of complex singularities for the 2D Euler equation, Physica D 219 (2006) 40–59.
[42] A.J. Chorin, The evolution of a turbulent vortex, Comm. Math. Phys. 83 (1982) 517–535.
[43] M.E. Brachet, D.I. Meiron, S.A. Orszag, B.G. Nickel, R.H. Morf, U. Frisch, Small-scale structure of the Taylor–Green vortex, J. Fluid Mech. 130 (1983) 411–452.
[44] E.D. Siggia, Collapse and amplification of a vortex filament, Phys. Fluids 28 (1984) 794–805.
[45] A. Pumir, E. Siggia, Collapsing solutions to the 3D Euler equations, Phys. Fluids A 2 (1990) 220–241.
[46] J.B. Bell, D.L. Marcus, Vorticity intensification and transition to turbulence in the three-dimensional Euler equations, Comm. Math. Phys. 147 (1992) 371–394.
[47] M.E. Brachet, V. Meneguzzi, A. Vincent, H. Politano, P.-L. Sulem, Numerical evidence of smooth self-similar dynamics and the possibility of subsequent collapse for ideal flows, Phys. Fluids 4A (1992) 2845–2854.
[48] R.M. Kerr, Evidence for a singularity of the three-dimensional incompressible Euler equations, Phys. Fluids A 5 (1993) 1725–1746.
[49] R.M. Kerr, Vorticity and scaling of collapsing Euler vortices, Phys. Fluids A 17 (2005) 075103–075114.
[50] O.N. Boratav, R.B. Pelz, Direct numerical simulation of transition to turbulence from a high-symmetry initial condition, Phys. Fluids 6 (1994) 2757–2784.
[51] O.N. Boratav, R.B. Pelz, On the local topology evolution of a high-symmetry flow, Phys. Fluids 7 (1995) 1712–1731.
[52] R.B. Pelz, Locally self-similar, finite-time collapse in a high-symmetry vortex filament model, Phys. Rev. E 55 (1997) 1617–1626.
[53] R.B. Pelz, Y. Gulak, Evidence for a real-time singularity in hydrodynamics from time series analysis, Phys. Rev. Lett. 79 (1997) 4998–5001.
[54] R.B. Pelz, Symmetry and the hydrodynamic blow-up problem, J. Fluid Mech. 444 (2001) 299–320.
[55] C. Cichowlas, M.-E. Brachet, Evolution of complex singularities in Kida–Pelz and Taylor–Green inviscid flows, Fluid Dynam. Res. 36 (2005) 239–248.
[56] Y. Gulak, Richard B. Pelz, High-symmetry Kida flow: Time series analysis and resummation, Fluid Dynam. Res. 36 (2005) 211–220.
[57] R.B. Pelz, K. Ohkitani, Linearly strained flows with and without boundaries — the regularizing effect of the pressure term, Fluid Dynam. Res. 36 (2005) 193–210.
[58] R. Grauer, C. Marliani, K. Germaschewski, Adaptive mesh refinement for singular solutions of the incompressible Euler equations, Phys. Rev. Lett. 80 (1998) 4177–4180.
[59] T.Y. Hou, R. Li, Dynamic depletion of vortex stretching and non-blowup of the 3-D incompressible Euler equations, J. Nonlinear Sci. 16 (2006) 639–664.

[60] P. Orlandi, G. Carnevale, Nonlinear amplification of vorticity in inviscid interaction of orthogonal Lamb dipoles, Phys. Fluids 19 (2007) 057106.
[61] T.Y. Hou, Blowup or no blowup? The interplay between theory and numerics, Physica D 237 (14–17) (2008) 1937–1944.
[62] M.D. Bustamente, R.M. Kerr, 3D Euler in a 2D symmetry plane, Physica D 237 (14–17) (2008) 1912–1920.
[63] T. Grafke, H. Homann, J. Dreher, R. Grauer, Numerical simulations of possible finite time singularities in the incompressible Euler equations: Comparison of numerical methods, Physica D 237 (14–17) (2008) 1932–1936.
[64] P. Constantin, Geometric statistics in turbulence, SIAM Rev. 36 (1994) 73–98.
[65] P. Constantin, Singular, weak and absent: Solutions of the Euler equations, Physica D 237 (14–17) (2008) 1926–1931.
[66] P. Constantin, Ch. Fefferman, A. Majda, A. Geometric constraints on potentially singular solutions for the 3D Euler equation, Comm. Partial Differential Equations 21 (1996) 559–571.
[67] D. Cordoba, Ch. Fefferman, On the collapse of tubes carried by 3D incompressible flows, Comm. Math. Phys. 222 (2001) 293–298.
[68] J. Deng, T.Y. Hou, X. Yu, Geometric properties and non-blowup of 3D incompressible Euler flow, Comm. Partial Differential Equations 30 (2005) 225–243.
[69] J. Deng, T.Y. Hou, X. Yu, Improved geometric condition for non-blowup of the $3D$ incompressible Euler equation, Comm. Partial Differential Equations 31 (2006) 293–306.
[70] B. Hoskins, M. McIntyre, A.W. Robertson, On the use and significance of isentropic potential vorticity maps, Quart. J. Roy. Met. Soc. 111 (1985) 877–946.
[71] H. Ertel, Ein Neuer Hydrodynamischer Wirbelsatz, Met. Z. 59 (1942) 271–281.
[72] C. Truesdell, R.A. Toupin, Classical field theories, in: S. Flugge (Ed.), Encyclopaedia of Physics III/1, Springer, 1960.
[73] E. Kuznetsov, V.E. Zakharov, Hamiltonian formalism for nonlinear waves, Phys. Uspekhi 40 (1997) 1087–1116.
[74] A. Viudez, On Ertel's potential vorticity theorem. On the impermeability theorem for potential vorticity, J. Atmos. Sci. 56 (1999) 507–516.
[75] S. Klainerman, 1984, unpublished.
[76] K. Ohkitani, Eigenvalue problems in three-dimensional Euler flows, Phys. Fluids A 5 (1993) 2570–2572.
[77] K. Ohkitani, S. Kishiba, Nonlocal nature of vortex stretching in an inviscid fluid, Phys. Fluids A 7 (1995) 411–421.
[78] J.D. Gibbon, D.D. Holm, Lagrangian particle paths and ortho-normal quaternion frames, Nonlinearity 20 (2007) 1745–1759.
[79] J. Léorat, Thèse de Doctorat, Université Paris-VII, 1975.
[80] P. Vieillefosse, Internal motion of a small element of fluid in an inviscid flow, Physica A 125 (1984) 150–162.
[81] E.A. Novikov, Internal dynamics of flows and formation of singularities, Fluid Dynam. Res. 6 (1990) 79–89.
[82] B.J. Cantwell, Exact solution of a restricted Euler equation for the velocity gradient tensor, Phys. Fluids 4 (1992) 782–793.
[83] S. Girimaji, C. Speziale, A modified restricted Euler equation for turbulent flows with mean velocity gradients, Phys. Fluids 7 (1995) 1438–1446.
[84] A. Ooi, J. Martin, J. Soria, M.S. Chong, A study of the evolution and characteristics of the invariants of the velocity-gradient tensor in isotropic turbulence, J. Fluid Mech. 381 (1999) 141–174.
[85] J. Martin, A. Ooi, A., M. Chong, J. Soria, Dynamics of the velocity gradient tensor invariants in isotropic turbulence, Phys. Fluids 10 (1998) 2336–2346.
[86] A. Naso, A. Pumir, Scale dependence of the coarse-grained velocity derivative tensor structure in turbulence, Phys. Rev. E 72 (2005) 056318–056326.
[87] P. Constantin, Note on loss of regularity for solutions of the 3D incompressible Euler and related equations, Comm. Math. Phys. 104 (1986) 311–326.
[88] M. Chertkov, A. Pumir, B.I. Shraiman, Lagrangian tetrad dynamics and phenomenology of turbulence, Phys. Fluids 11 (1999) 2394–2410.
[89] L. Chevillard, C. Meneveau, Lagrangian dynamics and statistical geometric structure of turbulence, Phys. Rev. Lett. 97 (2006) 174501–174504.
[90] G. Falkovich, K. Gawedzki, M. Vergassola, Particles and fields in fluid turbulence, Rev. Modern Phys. 73 (2001) 913–975.
[91] A. La Porta, G.A. Voth, A. Crawford, J. Alexander, E. Bodenschatz, Fluid particle accelerations in fully developed turbulence, Nature 409 (2001) 1017–1019.
[92] N. Mordant, J.F. Pinton, Measurement of Lagrangian velocity in fully developed turbulence, Phys. Rev. Lett. 87 (2001) 214501–214504.
[93] G.A. Voth, A. La Porta, A. Crawford, E. Bodenschatz, J. Alexander, Measurement of particle accelerations in fully developed turbulence, J. Fluid Mech. 469 (2002) 121–160.
[94] N. Mordant, A.M. Crawford, E. Bodenschatz, Three-dimensional structure of the Lagrangian acceleration in turbulent flows, Phys. Rev. Lett. 93 (2004) 214501–214504.
[95] N. Mordant, E. Leveque, J.F. Pinton, Experimental and numerical study of the Lagrangian dynamics of high Reynolds turbulence, New J. Phys. 6 (2004) 116–160.
[96] B.A. Lüthi, A. Tsinober, W. Kinzelbach, Lagrangian measurement of vorticity dynamics in turbulent flow, J. Fluid Mech. 528 (2005) 87–118.
[97] L. Biferale, G. Boffetta, A. Celani, A. Lanotte, F. Toschi, Particle trapping in three-dimensional fully developed turbulence, Phys. Fluids 17 (2005) 021701–021704.
[98] A.M. Reynolds, N. Mordant, A.M. Crawford, E. Bodenschatz, On the distribution of Lagrangian accelerations in turbulent flows, New J. Phys. 7 (2005) 58–67.
[99] W. Braun, F. De Lillo, B. Eckhardt, Geometry of particle paths in turbulent flows, J. Turbulence 7 (2006) 1–10.
[100] J.D. Gibbon, Ortho-normal quaternion frames, Lagrangian evolution equations and the three-dimensional Euler equations, Uspekhi Mat. Nauk 62 (3) (2007) 47–72. In English Russian Math. Surveys 62 (3) (2007) 1–26.
[101] J.D. Gibbon, D.D. Holm, R.M. Kerr, I. Roulstone, Quaternions and particle dynamics in Euler fluid flow, Nonlinearity 19 (2006) 1969–1983.
[102] J.D. Gibbon, A quaternionic structure in the three-dimensional Euler and ideal magneto-hydrodynamics equation, Physica D 166 (2002) 17–28.
[103] B. Galanti, J.D. Gibbon, M. Heritage, Vorticity alignment results for the 3D Euler and Navier–Stokes equations, Nonlinearity 10 (1997) 1675–1695.
[104] J. O'Connor, E. Robertson, Sir William Rowan Hamilton. http://www-groups.dcs.st-and.ac.uk/history/.
[105] P.G. Tait, An Elementary Treatise on Quaternions, 3rd ed., Cambridge University Press, Cambridge, 1890.
[106] W.R. Hamilton, Elements of Quaternions, Cambridge University Press, Cambridge, Repub. Chelsea, 1969.
[107] J.B. Kuipers, Quaternions and Rotation Sequences: A Primer with Applications to Orbits, Aerospace, and Virtual Reality, Princeton University Press, Princeton, 1999.
[108] A.J. Hanson, Visualizing Quaternions, Morgan Kaufmann Elsevier, London, 2006.
[109] K. Shoemake, Animating rotation with quaternion curves, in: Computer Graphics, SIGGRAPH Proceedings 19 (1985) 245–254.
[110] E.T. Whittaker, A Treatise on the Analytical Dynamics of Particles and Rigid Bodies, Dover, New York, 1944.
[111] V.I. Arnold, Mathematical methods of Classical Mechanics, Springer Verlag, Berlin, 1978.
[112] J.E. Marsden, Lectures on geometric methods in mathematical physics, in: CBMS-NSF Regional Conference Series in Applied Mathematics, vol. 37, SIAM, Providence, 1981.
[113] J.E. Marsden, Lectures on Mechanics, Cambridge University Press, Cambridge, 1992.
[114] D.D. Holm, Geometric Mechanics, Part II: Rotating, Translating and Rolling, Imperial College Press, London, 2007 (in press).
[115] Y. Brenier, Minimal geodesics on groups of volume-preserving maps and generalized solutions of the Euler equations, Comm. Pure Appl. Math. 52 (1999) 411–452.
[116] A. Shnirelman, On the non-uniqueness of weak solution of the Euler equation, Comm. Pure Appl. Math. 50 (12) (1997) 1261–1286.